A Valence Bond Study of the Bergman Cyclization: Geometric Features, Resonance Energy, and Nucleus-Independent Chemical Shift (NICS) Values

John Morrison Galbraith,[b] Peter R. Schreiner,*[a] Nathan Harris,[b] Wu Wei,[c] Alexander Wittkopp,[a] and Sason Shaik*[b]

In memoriam of Robert R. Squires

Abstract: The Bergman cyclization of (*Z*)-hex-3-ene-1,5-diynes (**1**, enediynes), which produces pharmacologically important DNA-cleaving biradicals (1,4-benzyne, **2**), was studied by using Hartree–Fock (HF) and density-functional theory (DFT) based valence bond (VB) methods (VB-HF and VB-DFT, respectively). We found that only three VB configurations are needed to arrive at results not too far from complete active space {CASSCF(6×6)} computations, while the quality of VB-DTF utilizing the same three configurations improves upon CASSCF(6×6) analogous to CASPT2. The dominant VB configuration in **1** contributes little to **2**, while the most important biradical configuration in **2** plays a negligible role in **1**. The avoided crossing of the energy curves of these two configurations along the reaction coordinate leads to the transition state (**TS**). As a consequence of the shape and position of the crossing section, the changes in geometry and in the electronic wavefunction along the reaction coordinate are non-synchronous; the **TS** is geometrically $\approx 80\,\%$ product-like and electronically $\approx 70\,\%$ reactant-like. While the π resonance in the **TS** is very small, it is large (64.4 kcal mol^{-1}) for **2** (cf. benzene = 61.5 kcal mol^{-1}). As a consequence, substituents operating on the σ electrons should be much more effective in changing the Bergman reaction cyclization barrier. Furthermore, additional σ resonance in **2** results in unusually high values for the nucleus-independent chemical shift (NICS, a direct measure for aromaticity). Similarly, the high NICS value of the **TS** is due mostly to σ resonance to which the NICS procedure is relatively sensitive.

Keywords: aromaticity · Bergman cyclization · computer chemistry · density functional calculations · valence-bond theory

Introduction

Enediyne natural products such as calicheamicin, dynemicin, and esperamicin are pharmacologically active through their ability to undergo Bergman cyclizations leading to the formation of *p*-benzyne biradical intermediates. These are able to abstract hydrogen atoms from DNA phosphodiester strands leading to cell death. Unfortunately, toxic side effects of enediyne-carrying drugs are severe so that an understanding of the factors governing the generation of these biradicals is essential for further drug development.[1] Chen and coworkers[2] have taken promising steps toward greater selectivity by modifications in the enediyne precursors. This type of approach requires a detailed knowledge of the reaction mechanism in order to engineer *p*-benzyne derivatives with the desired properties. However, uncovering such detail is not so straightforward; this is one of the aims of the present work.

The experimentally[2–19] and theoretically[8, 20–33] well-studied Bergman cyclization presents a prime example of a reaction in which the progression of the changes in the geometry and in the wavefunction along the reaction coordinate do not seem to coincide.[34–37] Thus, the geometry of the transition state (**TS**) for this endothermic (8.5 ± 1 kcal mol^{-1},[38] Scheme 1) ring closure of (*Z*)-hex-3-ene-1,5-diyne (enediyne **1**) appears from Scheme 1 to be product-like as generally expected from the Hammond postulate;[39] therefore, one might have expected also a significant biradical character in the **TS**. However, the activation barriers can be reproduced quite well with restricted single-determinant

[a] Priv.-Doz. Dr. P. R. Schreiner, A. Wittkopp
Institut für Organische Chemie
der Georg-August Universität
Tammannstrasse 2, 37077 Göttingen (Germany)
E-mail: pschrei@gwdg.de

[b] Prof. S. Shaik, Dr. J. M. Galbraith, N. Harris
The Department of Organic Chemistry and the Lise Meitner-Minerva Center for Computational Quantum Chemistry
Hebrew University
91904 Jerusalem (Israel)
E-mail: sason@yfaat.ch.huji.ac.il

[c] Prof. W. Wei
Department of Chemistry and State Key Laboratory for Physical Chemistry of Solid Surfaces
Xiamen University
Xiamen, 361005 (PR China)

0947-6539/00/0608-1446 $ 17.50+.50/0 *Chem. Eur. J.* **2000**, *6*, No. 8

Abstract in German: *Die Bergman-Cyclisierung von (Z)-Hex-3-en-1,5-diin (**1**, Endiin), die pharmakologisch aktive, DNA-spaltende Biradikale (1,4-Benzin, **2**) liefert, wurde mit Hilfe der Valenzbindungstheorie (VB-Theorie) auf dem Hartree-Fock- (HF) und Dichtefunktionaltheorie- (DFT) Niveau (VB-HF bzw. VB-DFT) untersucht. Man benötigt nur drei VB-Konfigurationen, um Ergebnisse zu erzielen, die denen von „complete active space" {CASSCF(6 × 6)} Rechnungen nur wenig nachstehen. Die dominante VB-Konfiguration in **1** trägt nur wenig zu **2** bei. Umgekehrt spielt die Biradikalkonfiguration von **2** in **1** eine untergeordnete Rolle. Das „avoided crossing" der Energiekurven dieser beiden Konfigurationen entlang der Reaktionskoordinate führt zum Übergangszustand (**TS**). Bedingt durch die Form und Lage der Überlappungsregion sind die Änderungen der Geometrie und der elektronischen Wellenfunktion nicht synchron; der **TS** ist geometrisch ≈80 % Produkt- elektronisch aber ≈70 % Edukt-artig. Während die π-Resonanz im **TS** sehr klein ist, ist sie in **2** groß (64.4 kcal mol^{-1}; zum Vergleich: Benzol = 61.5 kcal mol^{-1}). Folglich sollten Substituenten, welche auf die σ-Elektronen wirken, die Cyclisierungsbarriere der Bergman-Reaktion stärker beeinflussen als π-aktive Substituenten. Bedingt durch die erhöhte σ-Resonanz in **2** ergeben sich ungewöhnlich hohe „nucleus-independent chemical shift-" Werte (NICS, ein direktes Maß für Aromatizität). In ähnlicher Weise ist der hohe NICS-Wert des **TS** hauptsächlich auf σ-Resonanz zurückzuführen, worauf das NICS-Verfahren besonders empfindlich anspricht.*

Abstract in Hebrew:

תקציר: דחיסת ברגמן של אן-דיאנים **(1)** אשר יוצרת דירדיקלים (1,4-בנזאיין, **2**) בוקעי דנ״א נחקרה באופן תיאורטי בשיטות תורת הקשר הערכי (VB) המבוססות על קרובי הרטרי-פוק ופונקציונל-צפיפות. שלוש קונפיגורציות VB נידרשות לתת תוצאות קרובות ל-CASSCF(6*6). קונפיגורצית ה- VB הדומיננטית של **1** היא מינימלית עבור **2**, בעוד הקונפיגורציה הבי-רדיקלית החשובה ב- **2** זניחה ב-**1**. המנעות חציה של עקומות האנרגיה של שתי הקונפיגורציות הללו לאורך קואורדינטת התגובה אחראית ליצירת מצב המעבר. כתוצאה מהצורה והמיקום של אזור החציה, השינוים הגיאומטרים והאלקטרונים במצב המעבר אינם מתואמים. מצב המעבר מחונן באופי גיאומטרי שהוא בערך 80% דמוי-תוצר ואופי אלקטרוני שהוא בערך 70% דמוי מגיב. בעוד הרזוננס במערכת ה-π (רזוננס-π) במצב המעבר הינו מועט, הריהו גדול (64.4 קק״ל/מול) עבור התוצר **2** (אנרגית הרזוננס בבנזן היא 61.5 קק״ל/מול עבור אותם תנאי חישוב). אי לכן, אנו צופים שמתמירים בעלי השפעת σ יהיו יותר אפקטיבים בשינוי מחסום האנרגיה. יתרה מכך, עודף של רזוננס-σ בתוצר **2** נמצא תורם לערכי ניקס (NICS) גבוהים במיוחד (ניקס מהווה מדד לארומטיות). בדומה, מקורו של הניקס הגבוה המחושב עבור מצב המעבר נובע בעיקר מרזוננס-σ.

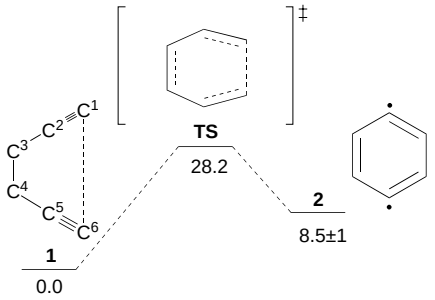

Scheme 1. The experimentally determined potential energy hypersurface for the Bergman cyclization from reference [27]; energies in kcal mol^{-1}.

wavefunctions[27] which suggests that while the **TS** may resemble the product (*p*-benzyne **2**) in geometry, it lacks the associated diradical character electronically. This disparity belongs to the general phenomenon of "non-perfect synchronization"[34–37, 40–42] observed, for example, in proton transfer between localized bases where resonance development in the **TS** appears to lag behind. The non-perfect synchronicity in the Bergman cyclization poses one problem we wish to address herein. This problem is also linked to the developing aromatic character[43, 44] in the transition structure which is expected to be small when considering energies, but reasonably large when one recognizes the geometric resemblance of the transition state to the aromatic product.

Further methodological difficulties arise because some of the enediyne π bonds transform into the *p*-benzyne σ framework perpendicular to the resulting aromatic π system. Thus, the electronic reorganization occurs in two planes (σ and π) and this complexity merits also some elucidation. The only means of resolving difficulties of this nature is through a balanced theoretical treatment that allows a clean separation of the in-plane development of the biradical character and the extent of out-of-plane π aromaticity. These and related problems of non-perfect synchronicity have not yet been addressed in detail and are the main focus of the present valence bond (VB) [45–49] treatment of the Bergman cyclization using traditional VB and a newly developed combination of VB[50] with density functional theory[51, 52] (VB-DFT).

Computational Methods

VB methods and AO basis sets: All VB calculations in the present work utilized the self-consistent field valence bond (VBSCF) approach in which all active orbitals participating in VB configurations are optimized in the field of doubly occupied inactive orbitals, by analogy to the complete active space self-consistent field (CASSCF)[53] procedure. In the usual application, the inactive orbitals are treated as doubly occupied molecular orbitals (MOs) taken from a Hartree–Fock (HF) calculation. Therefore, this procedure will be designated VB-HF.

Owing to the stringent computational requirements for the **TS** and **2**, we utilized the recently developed VB-DFT approach[50] based on the paired-permanent-determinant algorithm. [54] In VB-DFT the inactive orbitals are derived

from any chosen variant of DFT, for example, BLYP in this study,[55–57] and their energy includes the exchange and correlation contributions defined over the density of the inactive subshell. The active orbitals are then treated in a VB manner and optimized in the field of the DFT sub-shell. We shall refer to this situation as VB-DFT.

The VB orbitals can be kept strictly localized on their respective fragments corresponding to the traditional VB approach,[58] or can have small delocalization tails thus forming Coulson–Fischer (CF) orbitals.[59] This is similar to the approach taken in the generalized valence bond (GVB)[60] and spin-coupled valence bond (SCVB)[61–64] methods. In this manner, many of the contributions from classic ionic structures can be included in a single covalent-like configuration.[65, 66] The use of CF orbitals is more complete due to the inclusion of ionic terms; therefore, unless noted otherwise, all results reported herein utilized CF orbitals. The combination of localized (l) orbitals along with the VB-DFT approach leads to a description of the reaction potential energy surface most in line with experimental values. As a result, this combination was used for all energy evaluations and is designated as l-VB-DFT.

The 6-311G* basis set previously employed[27] for final energy evaluations proved to be computationally intractable for the VB methods used. Therefore, all VB-DFT computations utilized the 6-31G* basis set. However, this basis set was also found to be very demanding and led to no obvious improvement. As a result all VB-HF results were obtained with the 6-31G basis set. All VBSCF calculations were performed with the XIAMEN[67] program at the previously determined BLYP/6-31G* optimized geometries whereas all BLYP, CASSCF, and NICS calculations were computed with the GAUSSIAN94 suite of programs.[68]

For comparative purposes, we also computed the absolute magnetic shieldings, termed the "nucleus-independent chemical shifts" (NICS)[70] at selected points in space as a function of the electron density using the GIAO approach.[69, 70] The geometrical center of the ring's heavy atoms served as the most easily defined reference point. These isotropic chemical shifts yield information about ring currents and aromatic properties of molecules.[70] Following the convention, aromatic molecules have negative isotropic NICS, while antiaromatic molecules have positive values. The absolute magnitude of a negative NICS is approximately proportional to the aromatic stabilization energy. NICS values may also be computed for open-shell species and are thus justified in their application to apparent multi-determinant cases.[71]

VB configuration set: One set of active VB orbitals was created from the three in-plane molecular orbitals (MOs) involved in bond forming/breaking throughout the reaction resulting in the pairing patterns depicted in Scheme 2. While this pairing of electrons represents the possibility of in-plane σ as well as π bonding, for the sake of clarity all VB configurations in the plane of the molecule will carry the designation σ. The σ pairing between C^1-C^2, C^3-C^4, and C^5-C^6 is expected to be the dominant configuration in the reactant and therefore configurations of this type will be designated $\Phi_{\sigma R}$. On the other hand, the σ pairing between

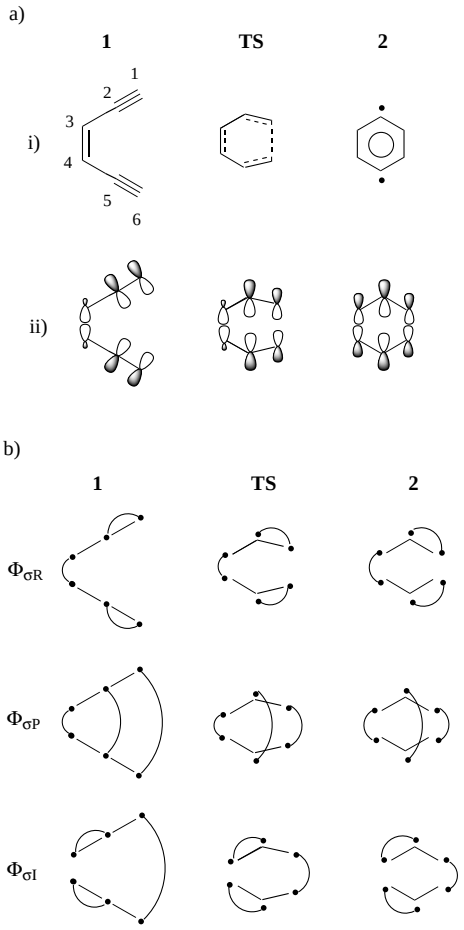

Scheme 2. VB pairing schemes for in-plane orbitals and bonds. Part a) shows two representations of **1**, **TS**, and **2** (Scheme 1): i) Lewis structures and ii) the active VB orbitals which participate in the σ bonding along the reaction coordinate. Both i) and ii) are depicted in the plane of the page. In b) we show the electron-pairing schemes of the active orbitals as depicted in ii) of part a) which were used herein.

C^1-C^6, C^2-C^5, and C^3-C^4 represents the singlet diradical character of the *p*-benzyne product **2** and thus will be designated $\Phi_{\sigma P}$. The pairing of C^1-C^6, C^2-C^3, and C^4-C^5 designated $\Phi_{\sigma I}$ is included from symmetry considerations, as it is necessary in order to properly describe the *p*-benzyne **2** but is expected to play only an intermediary role in the reaction (hence the subscript I). Thus, in the product **2**, $\Phi_{\sigma R}$ and $\Phi_{\sigma I}$ must be equivalent by symmetry, and both account for the through-bond delocalization of the diradical whose localized form is $\Phi_{\sigma P}$.

The possible π-pairing configurations are depicted in Scheme 3 in an analogous nomenclature to the σ configurations. The total wavefunction, designated as $\sigma+\pi$ is a product of the Φ_σ and Φ_π configurations. The inactive orbitals were held frozen after having been determined initially at the Hartree–Fock (HF) or BLYP levels for VB-HF or VB-DFT, respectively.

It should be noted that a complete description of a six-electron–six-center singlet system requires five unique VB configurations[72] and therefore, the above pairing schemes are incomplete. The missing σ configurations are the two additional cross-molecule Dewar-type pairings C^1-C^4, C^2-C^3,

0947-6539/00/0608-1448 $ 17.50+.50/0 *Chem. Eur. J.* **2000**, *6*, No. 8

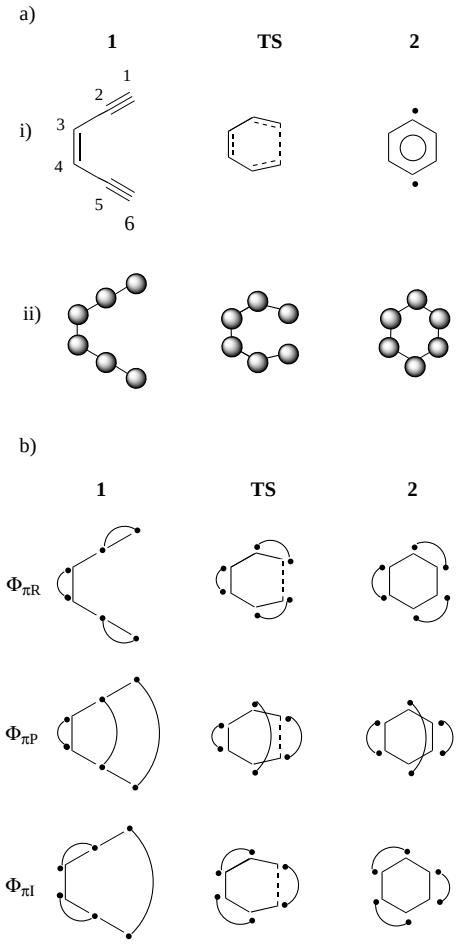

Scheme 3. VB pairing schemes for out-of-plane π electrons. Part a) shows two representations of **1**, **TS**, and **2** (Scheme 1): i) Lewis structures, and ii) the active VB orbitals which participate in π bonding along the reaction coordinate. In ii) only the top lobe of the π orbitals on each carbon is shown. In b) the molecule is represented in the plane of the page and all electron pairings involve only the π active orbitals as depicted in ii) of part a).

C^5-C^6 and C^1-C^2, C^3-C^6, C^4-C^5 (Scheme 4). Trial calculation of **2** where the Dewar structures would make the most difference show that $\Phi_{\sigma D1}$ and $\Phi_{\sigma D2}$ (Scheme 4a) contribute less than 0.3 kcal mol^{-1} when included in the σ-VB-HF calculation, thus justifying their exclusion.

On the other hand, the corresponding π-Dewar-type pairings $\Phi_{\pi D1}$ and $\Phi_{\pi D2}$ (Scheme 4b) are expected to be more important. However, including every possible σ and π combination from Schemes 2 and 3 along with the two additional π-Dewar-type configurations is exceedingly cumbersome (15 configurations). Neglect of $\Phi_{\sigma R}$ and $\Phi_{\sigma I}$ from the σ + π-VB-HF calculation costs only 0.2 kcal mol^{-1}. Thus, by inclusion of all π configurations listed in Scheme 3 along with $\Phi_{\pi D1}$ and $\Phi_{\pi D2}$ (Scheme 4b) combined with only the major σ contributor, $\Phi_{\sigma P}$, for a total of five configurations, it was possible to estimate the effect of the Dewar structures $\Phi_{\pi D1}$ and $\Phi_{\pi D2}$ as 2.5 kcal mol^{-1}.

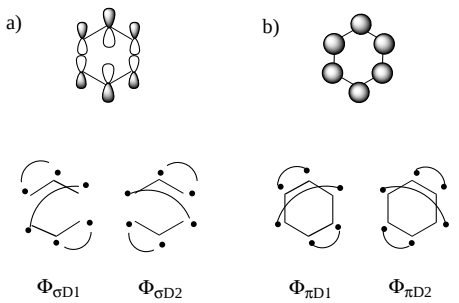

Scheme 4. Extra Dewar-type configurations of *p*-benzyne (**2**). a) active σ VB orbitals followed by pairings; b) active π VB orbitals (upper lobe only) followed by pairings. In each case the molecule is in the plane of the page.

Computing resonance energies: VB methods provide a means of calculating the resonance energy (RE) by comparing the energy of the lowest configuration to the energy when all configurations are mixed together. Thus, the total resonance energy RE_T can be determined as in Equation (1) where $E_{\sigma+\pi}$ refers to the adiabatic (orbitals re-optimized) energy of the

$$RE_T = E_{\sigma+\pi} - E_{full} \quad (1)$$

combination of the dominant σ and π configurations ($\Phi_{\sigma R} + \Phi_{\pi R}$ for **1** and **TS**, and $\Phi_{\sigma P} + \Phi_{\pi R}$ for **2**; labeled as in Schemes 2 and 3). E_{full} is the total energy for the full configuration set. RE_T was found at the σ + π-VB-HF level. It is advantageous to consider the π RE alone for the *p*-benzyne product **2** due to the similarity to benzene. In analogy to Equation (1), the expression for RE_π is shown in Equation (2) where E_π represents the energy of the localized π configuration, $\Phi_{\pi R}$.

$$RE_\pi = E_\pi - E_{full} \quad (2)$$

For the determination of RE_π of **2**, the more stringent requirements of the π system prompted the addition of $\Phi_{\pi D1}$ and $\Phi_{\pi D2}$ in the manner discussed above. In each case, E_{full} was treated with CF orbitals which were allowed to delocalize over all nearest neighbors, while the reference configuration utilized constrained CF orbitals which were only allowed to delocalize over paired neighbors. This approach gives RE_π values in line with other methods (i.e., ≈60 kcal mol^{-1} for benzene). If RE_π is taken as the difference between the total energy and the diabatic state energy of the dominant configuration *with the same CF orbitals delocalized freely*, RE_π values of 21.5 and 20.2 kcal mol^{-1} are obtained for **2** and benzene, respectively, in line with the value of 22.0 kcal mol^{-1} for benzene determined in a similar manner by Cooper, Stuart, Gerratt, and Raimondi.[73]

Results

Energetics: The energetic relations between **1**, the **TS**, and **2** (relative to **1**) are shown in Table 1. Weights of VB configurations in accordance with Schemes 2 and 3 are shown graphically in Figure 1. It can be seen from Table 1 that the Bergman rearrangement surface is highly variable depending on the method used.[27] While σ-VB-HF (entry 1) yields the correct ordering of the surface, the barrier associated with the **TS** and overall the ΔE are overestimated by ≈15 kcal mol^{-1}. Inclusion of the π system (entry 2) slightly improves the

Table 1. Energies (in kcal mol^{-1}) relative to the enediyne reactant **1** on the Bergman cyclization PES.

Entry	Level	Reactant **1**	**TS**	Product **2**
1	σ-VB-HF	0.0	44.8	23.1
2	σ + π-VB-HF	0.0	43.1	28.2 (25.7)[a]
3[b]	σ-l-VB-DFT	0.0	46.6	10.1
4	σ-VB-DFT	0.0	44.4	− 7.4
5	CASSCF(6x6)	0.0	40.4	16.4
6	BLYP/6 – 31G	0.0	27.1	14.9
7	BLYP/6 – 31G*[27]	0.0	25.3	11.8
8	expt. [38]	0.0	28.2	8.5

[a] σ + π-VB-HF which includes all combinations of $\Phi_{\sigma P}$ and all Φ_{π} configurations depicted in Scheme 3 and the Dewar-type pairings $\Phi_{\pi D1}$ and $\Phi_{\pi D2}$ as shown in Scheme 4b. [b] Using strictly localized VB orbitals.

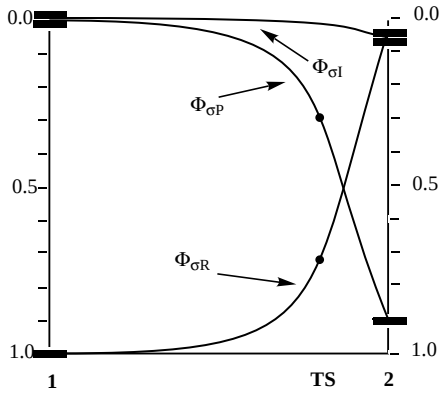

Figure 1. Weights of VB configurations. The plot is valid for all levels of theory employed herein (for σ + π methods, configuration labels refer to the σ pairing indicated as in Scheme 2 along with all π pairings from Scheme 3) Weights are ordered from 1.0 to 0.0 in order to complement Scheme 5.

energy of the **TS**, while the relative energy of **2** goes up. Regardless of whether only σ or σ + π orbitals are included in the configuration space, the barrier and overall reaction energy remain too high. Treating the π system of **2** in a delocalized manner results in further improvement. When only the σ system is treated by VB while the π system is kept delocalized as part of the HF MO core, the energy of **2** relative to **1** is lower than when the π system is treated by VB. In the language of classical VB theory, delocalization is achieved by adding ionic configurations which can also be accomplished by the use of CF orbitals.[65, 66] A further improvement can be made by including the other two Dewar-type structures (entry 2 in parentheses) which brings the relative energy of **2** down to 25.7 kcal mol^{-1}. On the other hand, the **TS** does not show such a preference for a delocalized treatment of the π system indicating the localized π nature of the **TS** as will be discussed below.

σ-l-VB-DFT (Table 1, entry 3) produces the best overall potential energy hypersurface due to inclusion of dynamic electron correlation which is essential for this type of problem.[21–27, 33, 74, 75] For VB-DFT the 6-31G* basis set was used, while for VB-HF we only utilized the 6-31G basis. The effect of adding polarization functions to the heavy atoms is relatively modest (3.1 kcal mol^{-1}; entries 6 and 7, Table 1) indicating that the improvement of σ-l-VB-DFT over VB-HF is not merely a basis set effect but is due to the advantage of the VB-DFT method.[50]

The VB-HF method is analogous to a CASSCF treatment in which the active space is chosen to include all MOs which can be constructed from every combination of the active VB orbitals.[65, 66] Thus a CASSCF(6 × 6) wavefunction should be similar to the σ-VB-HF wavefunction of the same dimension. σ-VB-HF yields a barrier which is slightly above the CASSCF(6 × 6) barrier, while the disagreement in the relative energies of **2** is more significant (6.7 kcal mol^{-1}). In fact, with such a small VB configuration set (only three configurations), it is remarkable that VB-HF performs roughly the same as CASSCF(6 × 6). One might say that VB-HF, like CASSCF, provides a qualitatively correct surface which still requires extensive dynamic correlation to give quantitative results.

This dynamic correlation is commonly included by some sort of perturbative addition to the CASSCF wavefunction by means of CASPT2[76, 77] or CASSCF(MP2).[78] Alternatively, some dynamic correlation effects can be introduced by VB-DFT which is only slightly more computationally demanding than VB-HF. As with σ-VB-HF, **TS** in σ-VB-DFT is slightly above the CASSCF(6 × 6) results, while **2** is 23.8 kcal mol^{-1} below those with CASSCF(6 × 6). Although employing a different active space, the CASPT2 results of Cramer[25] are similar in overstabilizing **2** relative to **1**. The advantage of the VB-DFT procedure lies in treating as much of the molecule as possible with DFT. Therefore, π orbitals were not included in the VB active space (i.e., σ + π-VB-DFT calculations). In addition, the results obtained with σ + π-VB-HF show that there is little advantage to including π electrons in the active space.

Weights of VB configurations: Despite the variation in relative energies among different methods, the weights of the VB configurations remain constant to within 0.05. Thus, the VB weights of all methods used herein can be represented uniformly as in Figure 1.

Discussion

The remarkable uniformity of the VB structural weights (even when the energetics vary considerably between methods, Table 1) makes it possible to draw conclusions about the origins of the barrier and the structure of the transition state. As expected, Figure 1 reveals that $\Phi_{\sigma R}$ is the dominant configuration in **1**, while $\Phi_{\sigma P}$ dominates **2**. A plot of the energies of these two VB configurations along the $C^1 - C^6$ distance leads to an avoided crossing giving rise to the **TS** as per the Shaik – Pross reactivity model[45–49] (Scheme 5). The crossing point is the point where these two configurations are in perfect resonance (have equal weights) and therefore has been termed the perfectly resonating state (PRS).[79] If there were no other configurations involved, the **TS** would be right at the PRS. However, Figure 1 and Table 2 indicate that the **TS** is approximately 0.70 $\Phi_{\sigma R}$ and 0.30 $\Phi_{\sigma P}$. The **TS** can be shifted away from the PRS by mixing in additional configurations such as $\Phi_{\sigma I}$ and associated ionic contributions. In addition, there are two other Dewar-type configurations which are not included in the VB manifold. Although these

0947-6539/00/0608-1450 $ 17.50+.50/0 *Chem. Eur. J.* **2000**, *6*, No. 8

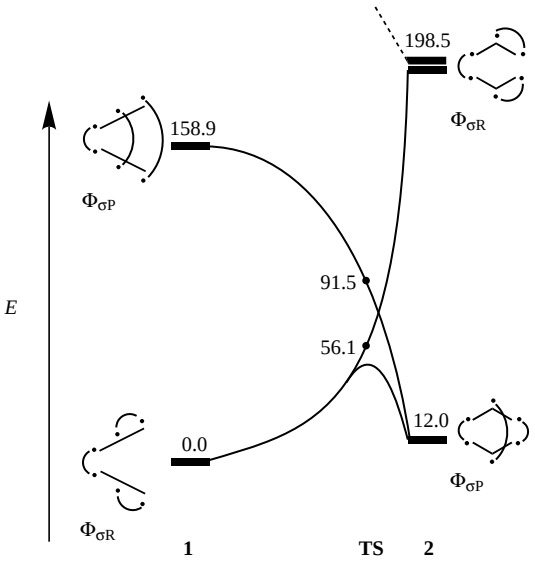

Scheme 5. VB curve crossing diagram showing the crossing of $\Phi_{\sigma R}$ and $\Phi_{\sigma P}$ (see Scheme 2b). Actual surface after mixing is shown as the continuous curve connecting $\Phi_{\sigma R}$ of **1** with $\Phi_{\sigma P}$ of **2**. Energies are in kcal mol^{-1} relative to the ground state of **1** at the σ-l-VB-DFT level. Mixing $\Phi_{\sigma P}$ with $\Phi_{\sigma R}$ and $\Phi_{\sigma I}$ results in the σ-l-VB-DFT energy of **2** as reported in entry 3 of Table 1.

Table 2. Progress of **TS** towards product **2**.

Entry	Property	Variable	Value[a]
1	electronic structure	$w_p \times 100$	≈ 30
2	geometry[b]	$\%\Delta \sphericalangle C^1\text{-}C^2\text{-}C^3$	79.9
3		$\%\Delta \sphericalangle C^2\text{-}C^3\text{-}C^4$	84.8
4		$\%\Delta C^1 - C^6$	80.7
5		$\%\Delta C^1 - C^2$	35.7
6		$\%\Delta C^2 - C^3$	20.0
7		$\%\Delta C^3 - C^4$	33.3

[a] Percentages (except for weights of VB configurations) are calculated from Equation (3). [b] BLYP/6–31G* geometries from reference[27].

two configurations are not explicitly involved in the VB calculation, the geometric placement of the **TS** was determined by the BLYP/6-31G* optimization procedure and therefore implicitly has the effects of all VB configurations built in.

This effect of the **TS** shifting away from the PRS has been discussed before,[79–81] and it was shown that small displacements from the crossing point may be accompanied by significant changes in the relative weights of the contributing configurations, depending on the shape of the curves in the avoided crossing region. Shaik et al. also pointed out that the region of the potential energy hypersurface (PES) including the **TS** and the PRS is extremely flat and therefore the PRS can be used as a chemically significant description of the **TS**.

Figure 2 shows a detailed portion of Scheme 5 in the avoided crossing region which was created by displacing the $C^1 - C^6$ distance from the **TS** geometry and optimizing all other parameters at the BLYP/6-31G* level. A σ-l-VB-DFT energy point was then calculated to determine energies and weights of VB configurations. Figure 2 indicates that the potential energy hypersurface in the avoided crossing region is indeed very flat with the PRS located at a $C^1 - C^6$ distance of 1.94 Å, 85.2 % along the way from **1** to **2** according to

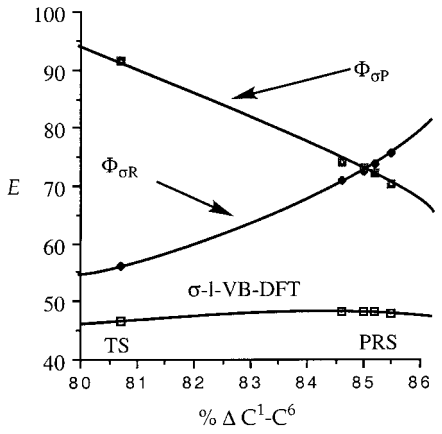

Figure 2. Details of the avoided crossing region at the σ-l-VB-DFT level. $\%\Delta C^1 - C^6$ distance determined by Equation (3). $C^1 - C^6$ distance is 2.08 Å at the **TS** (80.7 % $\Delta C^1 - C^6$) and 1.94 Å at the PRS (85.2 % $\Delta C^1 - C^6$). All energies in kcal mol^{-1} relative to the enediyne reactant **1**.

Equation (3) (vide infra), and very close to **TS** which is at 80.7 %. The σ-l-VB-DFT energy at the PRS is actually higher than at **TS** by < 2 kcal mol^{-1} indicating that while **TS** was determined at the BLYP/6-31G* level, the σ-l-VB-DFT TS may lie closer to the PRS. However, the PRS lies along the BLYP/6-31G* reaction coordinate and is not optimized for σ-l-VB-DFT. This along with the extreme flatness of the surface in the avoided crossing region precludes a definite conclusion concerning the precise relative energy of the PRS to the **TS**. Certainly, the PRS is a good approximation to the **TS**, and that the avoided crossing region defines also the **TS** region.

The BLYP/6-31G* geometries (for the coordinates see Supplementary Materials of ref.[27] at http://pubs.acs.org) reveal that the geometric parameters which undergo the greatest change throughout the reaction are $\sphericalangle C^1\text{-}C^2\text{-}C^3$ (52.8°) $\sphericalangle C^2\text{-}C^3\text{-}C^4$ (7.9°), and the $C^1 - C^6$ distance (3.06 Å) where the numbering refers to that in Scheme 1. These parameters can be applied to the simple reaction progress formula shown in Equation (3),[82] where ν is the progress variable, ρ is the

$$\nu_\rho = (\rho_r - \rho_{TS})/(\rho_r - \rho_p) \times 100\,\% \qquad (3)$$

geometric parameter in question; r, TS and p generically refer to the reactant, **TS**, and product, respectively. Accordingly, for these geometric parameters, the **TS** is ≈81 % product-like (Table 2). However, the $C^1 - C^2$, $C^2 - C^3$, and $C^3 - C^4$ bond lengths, which are associated with much higher force constants (than the above angle bending modes) and thus contribute a higher portion to the overall energy, are only about one-third product-like.

The extreme product-like character of the **TS** would appear to be in discord with Hammond's postulate[39] which states that when reactants and products are nearly equal in energy as in the present case (mildly endothermic with $\Delta H = 8.5 \pm 1$ kcal mol^{-1})[38] the **TS** should be geometrically only slightly product-like. Moreover, the product-like geometry of the **TS** is in contrast with the VB weights in Figure 1 which show the **TS** to be only about 30 % of the way towards the product (Table 2). While this is in accord with the $C^1 - C^2$ (entry 5), $C^2 - C^3$ (entry 6), and $C^3 - C^4$ (entry 7) bond lengths, these

parameters do not undergo major changes along the reaction coordinate and therefore are not good measures of the extent of reaction. Careful consideration of energetics associated with the geometric changes during reaction resolves this dilemma. Considering the fate of $\Phi_{\sigma R}$ on moving from reactant to product, for example, the energy curve of this state will rise very slowly at first, gradually becoming steeper and steeper (Scheme 5). This gradual energetic increase is due to the low cost of bending the $\measuredangle C^1$-C^2-C^3 angle. However, following $\Phi_{\sigma P}$ from product to reactant, the energy curve will climb steeply at first and taper off due to the initial high energy cost of breaking the C^1-C^6 bond. The result of such curved surfaces will weight the geometry of the $\Phi_{\sigma R}-\Phi_{\sigma P}$ crossing point in favor of the product **2**.

A further consequence of such a curvature among configurational energy surfaces is that a slight deviation from the crossing point due to mixing in of higher states will cause a dramatic separation of VB weights. In the present case, the crossing point of $\Phi_{\sigma R}$ and $\Phi_{\sigma P}$ which defines the PRS lies far towards the products in a geometric sense. Mixing of higher energy states moves the actual **TS** only slightly toward the reactant so that it remains geometrically predominantly product-like and close to the PRS. However, the sharp deviation in $\Phi_{\sigma R}$ and $\Phi_{\sigma P}$ in the vicinity of the crossing point leads to VB weights which show that the **TS** is electronically reactant-like. It is not uncommon to have a transition state which is geometrically similar to either reactant or product while electronically similar to the other.[83] In fact, as mentioned in the introduction, the imperfect synchronization of the progress parameters in the **TS** is quite a general phenomenon.[34–37] Our VB calculations show that the underlying electronic reason for this nonsynchronicity is the adjacency of the **TS** and the PRS and the curvature of the VB configurations which participate in the formation of the avoided crossing region.

Resonance energies: The π system can be considered separately from the σ system in order to gauge the extent of π aromaticity throughout the reaction (Table 3). In **2** $\Phi_{\pi R}$ and $\Phi_{\pi I}$ (Scheme 3) are equal while in **TS** one configuration will dominate over the other. The overall contribution from $\Phi_{\pi R}$ obtained by summing the weights of $\Phi_{\pi R}$ combined with all Φ_{σ} configurations is 0.95, showing that the π system is overwhelmingly reactant-like in the **TS** with little delocalization of π electrons. On the other hand, π delocalization in **2** is large. The RE_π of **2** as determined by Equation (2) is 64.4 kcal mol^{-1}, whereas that of benzene is only 61.5 kcal mol^{-1}.

To elucidate this point further, we assessed the relative aromatic character of **1**, the **TS**, **2**, and benzene by computing the NICS values at BLYP/6-31G*. In agreement with the RE_π analysis above, the NICS values (−28.8 for **2** and −9.3 for benzene at BLYP/6-31G*) also indicate that the product **2** is actually more aromatic than benzene. While the smaller average radius of the *p*-benzyne ring to that of benzene (1.40 Å versus 1.41 Å) would lead to a slightly larger NICS value, this does not account for such a large calculated discrepancy. In addition, the difference in RE_π [Eq. (2)] is smaller than NICS would indicate. This disagreement may originate from σ effects which certainly influence the NICS value. Indeed, our calculations reveal that there is considerable σ RE in **2** due to the mixing of $\Phi_{\sigma R}$ and $\Phi_{\sigma I}$ into $\Phi_{\sigma P}$ resulting in an RE_T value of 107.5 kcal mol^{-1}, determined by Equation (1). In MO parlance, the six electrons of the diradical, C^1-C^6, and C^3-C^4 bonds can be considered as a $4n+2$ σ aromatic system thus, endowing **2** with excess aromaticity and a larger NICS value than benzene. Considering the product **2** as a combination of fragments located on; a) C^1-C^6 and C^3-C^4 and b) C^2 and C^5 (Scheme 6) highlights the through-bond coupling interaction which mixes into the diradicaloid orbitals aAS (where "a" refers to fragment a and "AS" refers to antisymmetry or symmetry with respect to planes through the C^1-C^6 and C^3-C^4 bonds and C^2 and C^5, respectively).[84] The resulting MO is bonding between C^1, C^2, and C^3 and C^4, C^5, and C^6 leading to shortened bond lengths (1.36 Å as compared to 1.41 Å in benzene). Furthermore, this bond length is similar to the 1.37 Å C^3-C^4 bond length in **1**. In addition, this MO is antibonding between C^1-C^6 and C^3-C^4 leading to bonds which are long for a benzene-type system (1.49 Å) and on the order of a C–C single bond length.

Despite the dominance of a single π configuration in the **TS**, RE_T [Eq. (1)] is substantial (53.6 kcal mol^{-1}) and mostly due to the large RE_σ from the mixing of $\Phi_{\sigma R}$ and $\Phi_{\sigma P}$. Thus, the large NICS value for the **TS** (−18.8 kcal mol^{-1}) is due to σ rather than π aromaticity. The large π aromaticity of the product does not develop until a very advanced stage of the reaction despite the geometric similarities of the **TS** to **2**. It may seem contradictory that the **TS** has a higher NICS value than benzene when the RE_π of benzene is 61.5 kcal mol^{-1} and

Table 3. Resonance energies (in kcal mol^{-1}) on the potential energy hypersurface of the Bergman cyclization.[a]

	1	**TS**	**2**	Benzene
σ	21.8	29.8	43.1	–
π	14.0	23.8	64.4	61.5
Total	35.8	53.6	107.5	–
NICS	–	−18.8	−28.8	−9.3

[a] Determined by using Equations (1) and (2) at the σ + π-VB-HF level.

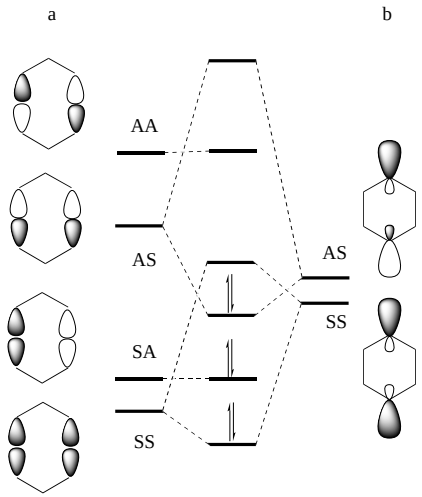

Scheme 6. Through-bond coupling in the *p*-benzyne product **2**. S and A refer to symmetry and antisymmetry with respect to planes bisecting the C^1-C^6 and C^3-C^4 bonds and going through C^2 and C^5, respectively.

0947-6539/00/0608-1452 $ 17.50+.50/0 *Chem. Eur. J.* **2000**, *6*, No. 8

the RE_T of the **TS** is only 53.6 kcal mol^{-1}. However, the point at which NICS is calculated is somewhat arbitrary and while the geometrical center of the heavy atom ring is the most easily definable as well as being the most transferable from system to system, this point will underestimate the π relative to σ ring current. Schleyer et al.[70, 85, 86] noted that this is due to the local paramagnetic contributions of the σ bonds which counteract the diamagnetic π-ring current effects. As the σ-system is not yet fully developed in the **TS**, the NICS value must be larger because of a smaller paratropic effect of the σ bonds.

The present example points out one of the dangers of indiscriminately using NICS as a gauge of aromaticity. Based on NICS alone, one might conclude that the Bergman cyclization goes through a transition state which is considerably more aromatic than benzene and due to geometric similarities to the *p*-benzyne product, this aromaticity must be a result of the π system. The true situation is quite different. The resonance stabilization in the **TS** is due mainly to the σ electrons and is actually *less* than the π-resonance energy in benzene. This is *not* to say that the NICS criterion is not useful to identify aromaticity but it is less suitable for a quantification of the relative degree of aromaticity.

Another aspect which demonstrates the electronic similarity of enediyne **1** and the transition structure is evident from the HOMO–LUMO gaps (ΔE). While the change in ΔE values from **1** to the **TS** is only 0.34 eV, the ΔE values of the **TS** and 1,4-didehydrobenzene (**2**) differ by 1.87 eV. Although the extrapolation of the orbital energies to the ionization energies is not straightforward in DFT,[87] the HOMO–LUMO gap is quantitatively related to chemical hardness and aromaticity. This analysis shows that the **TS** is essentially nonaromatic in the π sense, but has substantial σ-aromaticity. Strong aromaticity in conjunction with high polarizability and hence chemical softness[88] is observed in the biradical product **2**.

Conclusions

The ring closure of (*Z*)-hex-3-ene-1,5-diyne to 1,4-didehydrobenzene (the Bergman cyclization) is a reaction in which the out-of-plane π electrons play only a subsidiary role. The lowest energy π-electron configuration in the reactant develops smoothly to the products without crossing another configuration and is therefore barrierless. In this regard the Bergman cyclization is a [2 + 2] cycloaddition which is a symmetry-forbidden process. However, the through-bond coupling of the out-of-phase combination of the biradical centers makes this "forbidden" process allowed, but is associated with a considerable barrier.

The details of the Bergman cyclization **TS** are determined by the avoided crossing of the in-plane diyne, $\Phi_{\sigma R}$, and biradical, $\Phi_{\sigma P}$, electronic configurations. The shape of the energy curves for $\Phi_{\sigma R}$ and $\Phi_{\sigma P}$ along the reaction coordinate dictates the geometric placement of the crossing point (the perfectly resonating state, PRS) ≈85% towards the products. The shape of these curves also shows how even a slight shift away from the crossing point due to the mixing in of higher energy electron configurations leads to a **TS** which is electronically ≈30% product-like and ≈70% reactant-like, while remaining geometrically ≈80% product-like. This disparity between geometric and electronic changes along the reaction coordinate falls under the previously documented category of "non-perfect synchronization."[34–37, 40–42]

While the PRS and the **TS** do not lie at *exactly* the same point, they are within 0.2 Å of each other. In addition, the potential energy hypersurface is *extremely* flat in the avoided crossing region which therefore qualifies as the TS region. Shaik et al.[79–81] have proposed that the PRS can be taken as a chemically significant gauge of the transition state. The wealth of chemical information derived from the crossing point herein clearly supports this idea.

Total and π-resonance energies have been determined and compared to NICS values showing that the large discrepancy between the geometrically and electronically similar *p*-benzyne product and benzene is due to σ resonance in the *p*-benzyne. In addition, the transition state has a higher NICS value than benzene but lower π-resonance energy. Nearly all of the resonance energy in the transition state is attributed to the strong mixing of $\Phi_{\sigma R}$ and $\Phi_{\sigma P}$ in the avoided crossing region making the transition state "σ-aromatic". As a consequence, substituents operating on the σ framework should be most effective in altering the relative energies for the Bergman cyclization. While the total resonance energy of the transition state is smaller than the π-resonance energy of benzene, the NICS value is larger due to the underestimation of π-ring current when NICS is determined at the ring center which is a node in the π system. This example points out the arbitrary nature of the point at which NICS is calculated and calls for caution in using NICS as a gauge of aromaticity for structures that exhibit significant σ-ring currents.

Acknowledgements

The work at the Hebrew University was funded by the ISF established by the Israel Academy of Sciences and Humanities. J.M.G. is partially supported by the Lady Davis Fellowship Trust at the Hebrew University. N.H. is partially supported by a Fullbright Fellowship. This project was initiated during a visit of P.R.S. to the Lise Meitner-Minerva Center at the Hebrew University. The work in Göttingen was supported by the Fonds der Chemischen Industrie (Liebig-Fellowship for PRS), the Deutsche Forschungsgemeinschaft, and the Graduiertenförderung Niedersachsen. P.R.S. thanks Prof. A. de Meijere for his support and Matthias Prall for carefully reading the manuscript.

[1] A. M. Casazza, S. L. Kelly, *Enediyne Antibiotics as Antitumor Agents*, *Vol. 14*, Marcel Dekker, New York, **1995**.
[2] J. Hoffner, M. J. Schottelius, D. Feichtinger, P. Chen, *J. Am. Chem. Soc.* **1998**, *120*, 376–385.
[3] R. G. Bergman, *Acc. Chem. Res.* **1973**, *6*, 25–31.
[4] P. A. Carter, P. Magnus, *J. Am. Chem. Soc.* **1988**, *110*, 1626–1628.
[5] R. R. Jones, R. G. Bergman, *J. Am. Chem. Soc.* **1972**, *94*, 660–661.
[6] P. Magnus, S. A. Eisenbeis, R. A. Fairhurst, T. Iliadis, N. A. Magnus, D. Parry, *J. Am. Chem. Soc.* **1997**, *119*, 5591–5605.
[7] P. Magnus, R. T. Kewis, J. C. Huffman, *J. Am. Chem. Soc.* **1988**, *110*, 6921–6923.
[8] P. Magnus, S. Fortt, T. Pitterna, J. P. Snyder, *J. Am. Chem. Soc.* **1990**, *112*, 4986–4987.
[9] P. Magnus, R. A. Fairhurst, *J. Chem. Soc. Chem. Commun.* **1994**, 1541–1542.

[10] K. C. Nicolaou, G. Zuccarello, Y. Ogawa, E. J. Schweiger, T. Kumazawa, *J. Am. Chem. Soc.* **1988**, *110*, 4866 – 4868.
[11] K. C. Nicolaou, W.-M. Dai, *Angew. Chem.* **1991**, *103*, 1453 – 1481; *Angew. Chem. Int. Ed. Engl.* **1991**, *30*, 1387 – 1416.
[12] L. G. Paloma, J. A. Smith, W. J. Chazin, K. C. Nicolaou, *J. Am. Chem. Soc.* **1994**, *116*, 3697 – 3700.
[13] K. C. Nicolaou, W.-M. Dai, Y. P. Hog, S.-C. Tsay, K. K. Baldridge, J. S. Siegel, *J. Am. Chem. Soc.* **1993**, *115*, 7944 – 7953.
[14] P. Chen, *Angew. Chem.* **1996**, *108*, 1584 – 1586; *Angew. Chem. Int. Ed. Engl.* **1996**, *35*, 1478 – 1480.
[15] K. C. Nicolaou, P. Maligres, J. Shin, E. de Leon, D. Rideout, *J. Am. Chem. Soc.* **1990**, *112*, 7825 – 7826.
[16] M. J. Schottelius, P. Chen, *J. Am. Chem. Soc.* **1996**, *118*, 4896 – 4903.
[17] R. Gleiter, D. Kratz, *Angew. Chem.* **1993**, *105*, 884 – 887; *Angew. Chem. Int. Ed. Engl.* **1993**, *32*, 842 – 845.
[18] P. G. Wenthold, R. R. Squires, *J. Am. Chem. Soc.* **1994**, *116*, 6401 – 6412.
[19] P. G. Wenthold, R. R. Squires, W. C. Lineberger, *J. Am. Chem. Soc.* **1998**, *120*, 5279 – 5290.
[20] W.-H. Chen, N.-Y. Chang, C.-H. Yu, *J. Phys. Chem.* **1998**, *102*, 2584 – 2593.
[21] C. J. Cramer, J. J. Nash, R. R. Squires, *Chem. Phys. Lett.* **1997**, *277*, 311 – 320.
[22] R. Lindh, M. Schütz, *Chem. Phys. Lett.* **1996**, *258*, 409 – 4015.
[23] R. Lindh, T. J. Lee, A. Bernhardsson, B. J. Persson, G. Karlström, *J. Am. Chem. Soc.* **1995**, *117*, 7186 – 7194.
[24] N. Koga, K. Morokuma, *J. Am. Chem. Soc.* **1991**, *113*, 1907 – 1911.
[25] C. J. Cramer, *J. Am. Chem. Soc.* **1998**, *120*, 6261 – 6269.
[26] R. Lindh, B. J. Persson, *J. Am. Chem. Soc.* **1994**, *116*, 4963 – 4969.
[27] P. R. Schreiner, *J. Am. Chem. Soc.* **1998**, *120*, 4184 – 4190.
[28] J. P. Snyder, *J. Am. Chem Soc.* **1990**, *112*, 5367 – 5369.
[29] P. R. Schreiner, *Chem. Commun.* **1998**, 483 – 484.
[30] J. P. Snyder, G. E. Tipsword, *J. Am. Chem. Soc.* **1990**, *112*, 4040 – 4042.
[31] J. P. Snyder, *J. Am. Chem. Soc.* **1989**, *111*, 7630 – 7632.
[32] S. G. Wierschke, J. J. Nash, R. R. Squires, *J. Am. Chem. Soc.* **1993**, *115*, 11958 – 11967.
[33] E. Kraka, D. Cremer, *J. Am. Chem. Soc.* **1994**, *116*, 4929 – 4936.
[34] C. F. Bernasconi, P. J. Wenzel, *J. Am. Chem. Soc.* **1994**, *116*, 5405.
[35] C. F. Bernasconi, *Adv. Phys. Org. Chem.* **1992**, *27*, 119.
[36] W. J. Albery, C. F. Bernasconi, A. J. Kresge, *J. Phys. Org. Chem.* **1988**, *1*, 29.
[37] C. F. Bernasconi, *Acc. Chem. Res.* **1987**, *20*, 301.
[38] W. R. Roth, H. Hopf, C. Horn, *Chem. Ber.* **1994**, *127*, 1765 – 1769.
[39] G. S. Hammond, *J. Am. Chem. Soc.* **1955**, *77*, 334 – 338.
[40] N. Harris, W. Saunders, W. Wu, S. Shaik, *J. Phys. Org. Chem.* **1999**, *12*, 269.
[41] A. J. Kresge, *Chem. Soc. Rev.* **1973**, *2*, 475.
[42] A. J. Kresge, *Can. J. Chem.* **1974**, *52*, 1897.
[43] P. von R. Schleyer, H. Jiao, *Pure Appl. Chem.* **1996**, *68*, 209 – 218.
[44] P. J. Gerratt, *Aromaticity*, Wiley, New York, **1986**.
[45] A. Pross, S. S. Shaik, *Acc. Chem. Res.* **1983**, *16*.
[46] S. S. Shaik, *J. Am. Chem. Soc.* **1981**, *103*, 3692.
[47] A. Pross, *Adv. Phys. Org. Chem.* **1985**, *21*, 99.
[48] S. Shaik, A. C. Reddy, A. Ioffe, J. P. Dinnocenzo, D. Danovich, J. K. Cho, *J. Am. Chem. Soc.* **1995**, *117*, 3205 – 3222.
[49] S. Shaik, A. Shurki, *Angew. Chem.* **1999**, *111*, 616 – 657; *Angew. Chem. Int. Ed.* **1999**, *38*, 586.
[50] W. Wu, S. Shaik, *Chem. Phys. Lett.* **1999**, *301*, 37 – 42. This paper also addresses the issue of double-counting the electronic correlation energy at VB-DFT.
[51] W. Kohn, L. J. Sham, *Phys. Rev. A* **1965**, *140*, 1133 – 1143.
[52] P. Hohenberg, W. Kohn, *Phys. Rev. B* **1964**, *136*, 864 – 878.
[53] B. O. Roos, *Adv. Chem. Phys.* **1987**, *69*, 399 – 445.
[54] W. Wu, A. Wu, Y. Mo, M. Lin, Q. Zhang, *Int. J. Quant. Chem.* **1998**, *67*, 287.
[55] B. Miehlich, A. Savin, H. Stoll, H. Preuss, *Chem. Phys. Lett.* **1989**, *157*, 200.
[56] A. D. Becke, *Phys. Rev. A* **1988**, *38*, 3098 – 3100.
[57] C. Lee, W. Yang, R. G. Parr, *Phys. Rev.* **1988**, *37*, 785.
[58] L. Pauling, *The Nature of the Chemical Bond*, Cornell University Press, New York, **1960**.
[59] C. A. Coulson, I. Fischer, *Phil. Mag.* **1949**, *40*, 386.
[60] F. W. Bobrowicz, W. A. Goddard, *The Self-Consistent Field Equations for Generalized Valence Bond and Open-Shell Hartree-Fock Wavefunctions* (Ed.: H. F. Schaefer), *Modern Theoretical Chemistry: Methods of Electronic Structure Theory*, *Vol. 3*, Plenum, New York, **1977**, p. 79.
[61] D. L. Cooper, J. Gerratt, M. Raimondi, *Adv. Chem. Phys.* **1987**, *69*, 319.
[62] D. L. Cooper, J. Gerratt, M. Raimondi, *Int. Rev. Phys. Chem.* **1988**, *7*, 59.
[63] D. L. Cooper, J. Gerratt, M. Raimondi, *Advances in the Theory of Benzenoid Hydrocarbons* (Eds.: I. Gutman, S. J. Cyvin), Springer, Heidelberg, **1990**.
[64] D. L. Cooper, J. Gerratt, M. Raimondi, *Spin-Coupled Valence Bond Theory of Molecular Electronic Structure* (Eds.: D. J. Klein, N. Trinajstic), *Valence Bond Theory and Chemical Structure*, Elsevier, New York, **1990**, p. 287.
[65] P. C. Hiberty *J. Mol. Struct. (THEOCHEM)* **1998**, *451*, 237.
[66] P. C. Hiberty, D. L. Cooper *J. Mol. Struct. (THEOCHEM)* **1988**, *169*, 437.
[67] W. Wu, L. Song, Y. Mo, Q. Zhang, 1998, XIAMEN - An ab initio spin-free valence bond (VB) program, Xiamen University.
[68] M. J. Frisch, G. W. Trucks, H. B. Schlegel, P. M. W. Gill, B. G. Johnson, M. A. Robb, J. R. Cheeseman, T. Keith, G. A. Petersson, J. A. Montgomery, K. Raghavachari, M. A. Al-Laham, V. G. Zakrzewski, J. V. Ortiz, J. B. Foresman, J. Cioslowski, B. B. Stefanov, A. Nanayakkara, M. Challacombe, C. Y. Peng, P. Y. Ayala, W. Chen, M. W. Wong, J. L. Andres, E. S. Replogle, R. Gomperts, R. L. Martin, D. J. Fox, J. S. Binkley, D. J. Defrees, J. Baker, J. P. Stewart, M. Head-Gordon, C. Gonzalez, J. A. Pople, **1995**, Gaussian 94, Revision C.3, Pittsburgh PA, Gaussian, Inc.
[69] K. Wolinski, J. F. Hilton, P. Pulay, *J. Am. Chem. Soc.* **1990**, *112*, 8251 – 8260.
[70] P. von R. Schleyer, C. Maerker, A. Dransfeld, H. Jiao, N. J. R. van Eikema Hommes, *J. Am. Chem. Soc.* **1996**, *118*, 6317.
[71] V. Gogonea, P. von R. Schleyer, P. R. Schreiner, *Angew. Chem.* **1998**, *110*, 2045 – 2049; *Angew. Chem. Int. Ed.* **1998**, *37*, 1945 – 1948.
[72] R. Pauncz *Spin Eigenfunctions*, Plenum, London, **1979**. According to the rules of spin-pairing, any choice of five unique configurations will completely describe the system. The present choice is most closely related to chemical intuition and is most relevant throughout the reaction. Any other spin combination can be described by a linear combination of these five configurations.
[73] D. L. Cooper, S. C. Wright, J. Gerratt, M. Raimondi, *J. Chem. Soc. Perkin Trans. II* **1989**, 255.
[74] C. J. Cramer, *J. Phys. Chem. A* **1997**, *101*, 9191 – 9194.
[75] E. Kraka, D. Cremer, G. Bucher, H. Wandel, W. Sander, *Chem. Phys. Lett.* **1997**, *268*, 313 – 317.
[76] K. Andersson, B. O. Roos, *Multiconfigurational Second-Order Perturbation Theory* (Ed.: D. R. Yarkony), *Modern Electronic Structure Theory I*, World Scientific, Singapore, **1995**, pp. 55 – 109.
[77] K. Andersson, B. O. Roos, *Int. J. Quantum. Chem.* **1993**, *45*, 591.
[78] J. J. McDouall, K. Peasley, M. A. Robb, *Chem. Phys. Lett.* **1988**, *148*, 183.
[79] A. Shurki, S. Shaik, *J. Mol. Struct. (THEOCHEM)* **1998**, *424*, 37.
[80] S. Shaik, A. C. Reddy, *J. Chem. Soc. Faraday Trans.* **1994**, *90*, 1631.
[81] S. Shaik, A. Ioffee, A. C. Reddy, A. Pross, *J. Am. Chem. Soc.* **1994**, *116*, 262.
[82] S. S. Shaik, H. B. Schlegel, S. Wolfe, *Theoretical Aspects of Physical Organic Chemistry. The SN2 Mechanism*, Wiley, New York, **1992**.
[83] P. R. Schreiner, P. von R. Schleyer, H. F. Schaefer III, *J. Org. Chem.* **1997**, *62*, 4216 – 4228.
[84] R. Hoffmann, *Acc. Chem. Res.* **1974**, *1*, 1.
[85] T. K. Zywietz, H. Jiao, P. von R. Schleyer, A. de Meijere, *J. Org. Chem.* **1998**, *63*, 3417 – 3422.
[86] P. von R. Schleyer, H. Jiao, N. J. R. van Eikema-Hommes, V. G. Malkin, O. L. Malkina, *J. Am. Chem. Soc.* **1997**, *119*, 12669 – 12670.
[87] P. K. Chattaraj, P. von R. Schleyer, *J. Am. Chem. Soc.* **1994**, *116*, 1067 – 1071.
[88] Z. Zhou, R. G. Parr, *J. Am. Chem. Soc.* **1989**, *111*, 7371 – 7379.

Received: April 27, 1999 [F1751]

  0947-6539/00/0608-1454 $ 17.50+.50/0